

## Identification of coronaviruses by the use of indirect protein A-gold immunoelectron microscopy

Serge Dea, Simon Garzon

**Abstract.** Concentration by airfuge and protein A-colloidal gold immunoelectron microscopy (PAG-IEM) offered a rapid and sensitive method for detection and identification of coronaviruses from various species. The method was applied to partially purified tissue culture-adapted or egg-adapted mammalian and avian coronaviruses and to clarified fecal samples from diarrheic calves and turkey poult for detection of enteric coronaviruses. Aggregates of virus coated with specific antibody were seen in virus samples mixed with homologous antiserum but not in control samples containing preexposure serum. At least a 10-50-fold enhancement of the sensitivity of direct EM for virus detection was obtained using protein A-colloidal gold complex as an electron-dense marker. The PAG-IEM method demonstrated low nonspecific background labeling and permitted detection of soluble and particle-associated antigen. Reciprocal cross-reactivity was detected among the subgroup of mammalian hemagglutinating coronaviruses, and antisera to 4 members of other subgroups only recognized their homologous virus.

Coronaviruses, particularly enteropathogenic strains, from avian and mammalian species are difficult to grow in cell cultures.<sup>2,6</sup> Direct electron microscopy (DEM) of viral particles in clarified fecal specimens and fluorescent antibody techniques for detection of coronavirus antigens in the cells of infected gut are generally used for the diagnosis of enteric coronaviral infections.<sup>11,14,18,19,21</sup> The detection of coronavirus antigens by indirect immunofluorescence (IFF) is dependent on tissue being removed very shortly after death, and most antigen is present early in the course of disease.<sup>19,21</sup> The lack of highly specific antisera can also compromise the specificity of the IFF technique. Coronaviruses are difficult to identify in negatively stained preparations because they are very pleomorphic and the peplomers are lost during processing of clinical specimens.<sup>10,11,14</sup> It is difficult to distinguish coronavirus particles from cell artifacts such as parts of nuclear or cytoplasmic membranes and other fringed bodies.<sup>10</sup> Several immunoelectron microscopy (IEM) methods for detecting enteric coronaviruses are more sensitive than conventional DEM techniques;<sup>17,24</sup> however, the sensitivity of these methods is still dependent on the morphologic identification of virus particles or immune complexes on the EM grids. The recently described colloidal gold immunoelectron mi-

croscopy technique improves detection of bovine enteric coronavirus (BCV) in fecal samples.<sup>9</sup>

The purpose of the present study was to evaluate the efficiency of combining the concentration of viral suspensions by airfuge and the indirect protein A-colloidal gold immunoelectron microscopy labeling (PAG-IEM) techniques for the detection and differentiation of avian and mammalian enteric and respiratory coronaviruses.

### Materials and methods

**Viruses and cells.** Turkey and bovine enteric coronaviruses (TCV, BCV), porcine hemagglutinating encephalomyelitis virus (HEV), porcine transmissible gastroenteritis virus (TGEV), human HCV-OC43 and HCV-229E respiratory coronaviruses, mouse hepatitis virus (MHV), and 3 serotypes of avian infectious bronchitis virus (IBV) were used in the study. (The prototype egg-adapted Minnesota strain<sup>23</sup> of TCV was kindly supplied to us by B. S. Pomeroy.<sup>a</sup>) The virus was serially propagated in the presence of trypsin<sup>b</sup> in HRT-18 cells, a cell line derived from human rectal adenocarcinoma, as described previously.<sup>6</sup> The Mebus strain of BCV, strain 67N of HEV, the Purdue strain of TGEV, and serotype 3 of virus MHV were obtained from the ATCC.<sup>c</sup> These viruses were grown respectively in HRT-18, ST (swine testicle), and L2 (mouse fibroblasts) cells, as described previously.<sup>7</sup> The Beaudette, Holland, and Connecticut strains of IBV were propagated by inoculation into embryonating hen eggs.<sup>5</sup>

**Virus purification.** Viruses were purified from the supernatants of infected cell cultures, the clarified allantoic fluids, or the intestinal contents of infected embryonating eggs by differential and isopycnic ultracentrifugation on sucrose gradients.<sup>5,6</sup>

**Anti-coronavirus hyperimmune serum.** Anti-TCV hyperimmune serum was obtained after immunization of rabbits

From the Center for Research in Virology, Institute Armand-Frappier, University of Quebec, PO Box 100, Laval, PQ H7N 4Z3, Canada (Dea), and the Department of Microbiology, Faculty of Medicine, University of Montreal, Montreal, PQ H3C 3J7, Canada (Garzon).

Presented at the 33rd Annual Meeting of the AAVLD, Denver, CO, October 6-11, 1990.

Received for publication February 13, 1991.

with the purified egg-adapted Minnesota strain. The specificity of the antiserum has been confirmed by IEM and hemagglutination-inhibition tests.<sup>5</sup> Rabbit antisera to tissue culture-adapted BCoV, IBV, TGEV, HEV, and MHV-3 viruses were also produced.<sup>5,7</sup> The specificity of each antiserum was confirmed by IEM and seroneutralization.<sup>3</sup>

**Direct electron microscopy (DEM).** Aliquots (10  $\mu$ l) from clarified fecal specimens and clarified infected-cell culture fluids and fractions from sucrose gradients were spotted on formvar-carbon-coated grids and stained negatively with 2% sodium phosphotungstate (pH 7.0) as previously described.<sup>3</sup> The grids were examined on a Philips EM 300 electron microscope<sup>4</sup> at a potential of 80 kV.

**Protein A-gold immunolabeling electron microscopy (PAG-IEM).** Aliquots (100  $\mu$ l) of purified viral preparations or clarified fecal specimens (diluted 1:20) were poured into 240- $\mu$ l nitrocellulose microtubes<sup>5</sup> and concentrated by airfuge ultracentrifugation at 120,000  $\times$  g (30 psi) for 10 min onto 400-mesh naked-nickel grids. For immunogold labeling, virus-coated grids were washed 3 times in TBS (20 mM Tris, 150 mM NaCl, pH 7.2) partly dried, and floated for 5 min on a drop of TBS-T (TBS supplemented with 0.05% Tween 20). The grids were then incubated for 10 min at room temperature on a drop of rabbit hyperimmune serum (diluted 1:250) in TBS-T. Following another washing step, grids were incubated on a drop of TBS-diluted protein A-gold (PAG) complex. The colloidal gold particles in the PAG complex were 8 or 15 nm in diameter and were prepared as previously described,<sup>12</sup> with modifications.<sup>8</sup> The grids were finally washed with TBS, rinsed 3 times in distilled water, and counterstained with 2% sodium phosphotungstate, pH 7.0. Specificity of the labeling was demonstrated by controls, including nonimmune sera and incubation with PAG complex alone.

**Enzyme-linked immunosorbent assays (ELISA).** The double-antibody sandwich form of ELISA used for the detection of viruses in fecal samples has been described elsewhere.<sup>5</sup>

**Clinical specimens.** Intestinal contents from 1-8-wk-old turkey poults with mild to severe diarrhea were obtained from 38 commercial flocks located in southern Quebec.<sup>5</sup> Specimens from 5-10 poults from the same flock were pooled, and 1-2 g were homogenized in 10-20 ml of TBS buffer (pH 8.0) and clarified by centrifugation<sup>4</sup> at 5,000  $\times$  g for 30 min at 4 C. Supernatants were passed through membrane filters of 450-nm pore size and frozen at -70 C until used. Twenty fecal samples from 1-2-wk-old diarrheic calves were obtained from 12 dairy herds in southern Quebec that had experienced repeated outbreaks of neonatal calf diarrhea dur-

ing the last 2-3 yr. Specimens from diarrheic calves were processed as described above.<sup>3</sup>

## Results

### DEM and PAG-IEM of various coronaviruses

All initial experiments were done with concentrated viral preparations of each coronavirus in which the density of virions was sufficiently high to permit detection by DEM. Following incubation with preimmune serum, no clumping or only small clumps of 2-5 viral particles were observed with these preparations.

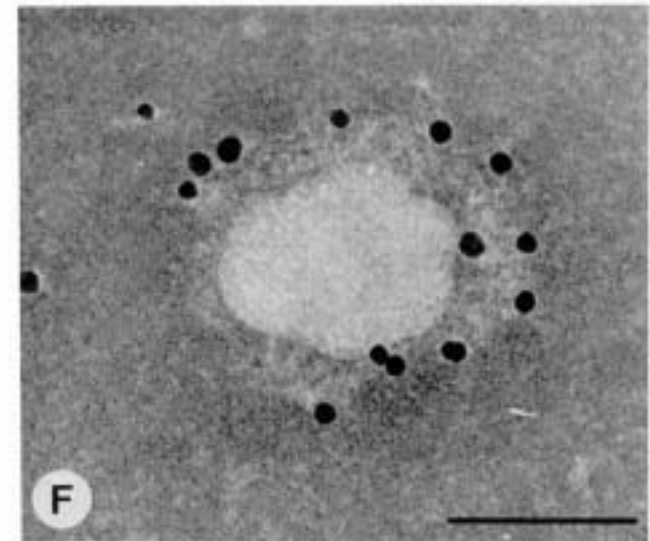
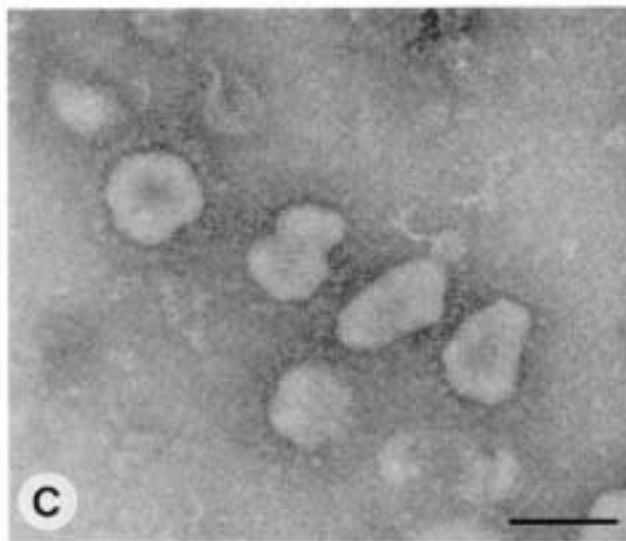
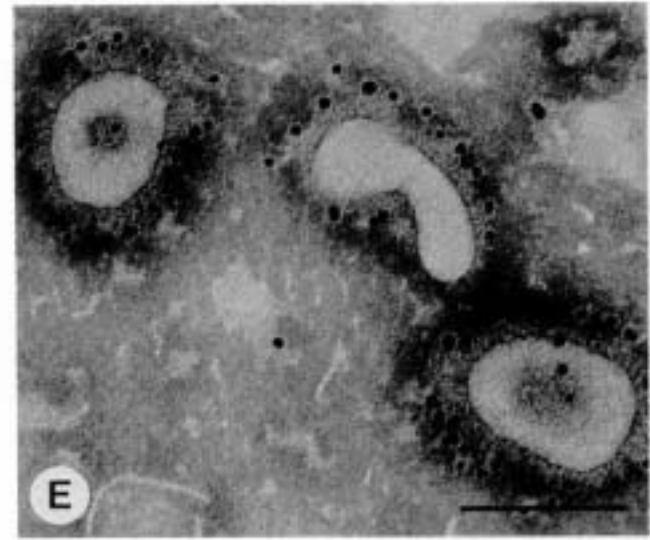
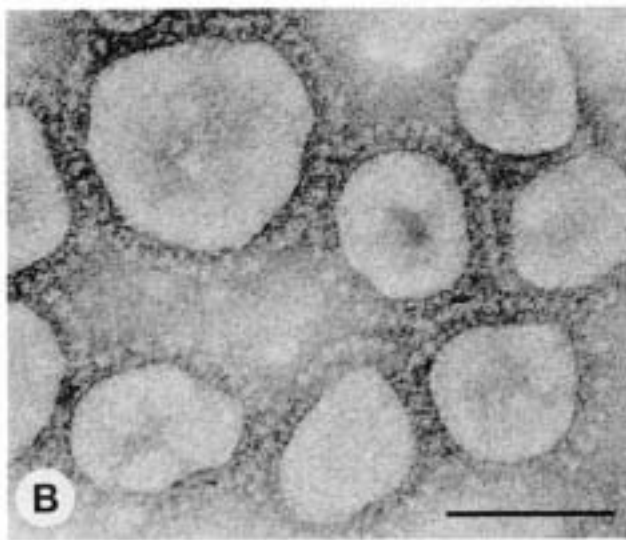
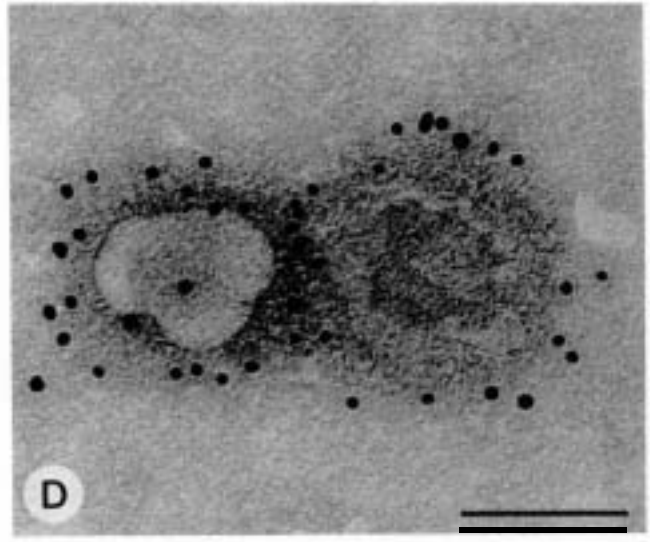
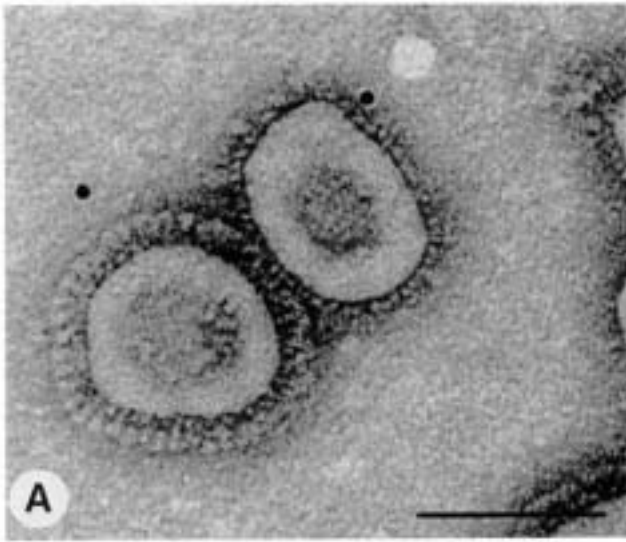
The virions of all coronaviruses used in this study were moderately pleomorphic but mostly spherical, with a diameter ranging between 60 to 220 nm (Figs. 1, 2). Most particles were centrally depressed (dark staining center) and surrounded by a fringe of well-defined regularly spaced petal-shaped or club-shaped projections 12-20 nm long. In all cases, the peplomers were always larger in diameter at the distal end than at the site of attachment to the virions.

A second fringe of small granular projections located near the base of the more typical coronaradiations could be distinguished in cases of BCoV, HCoV-OC43, and HEV, 3 viruses classified serologically in the subgroup of hemagglutinating mammalian coronaviruses (Figs. 1A, 2B, 2C).<sup>16</sup> These additional granular projections were particularly well defined on those particles that lost their larger more typical coronaradiations during processing (Fig 1A). The TCV virions also possessed 2 types of surface projections (Fig. 1B).

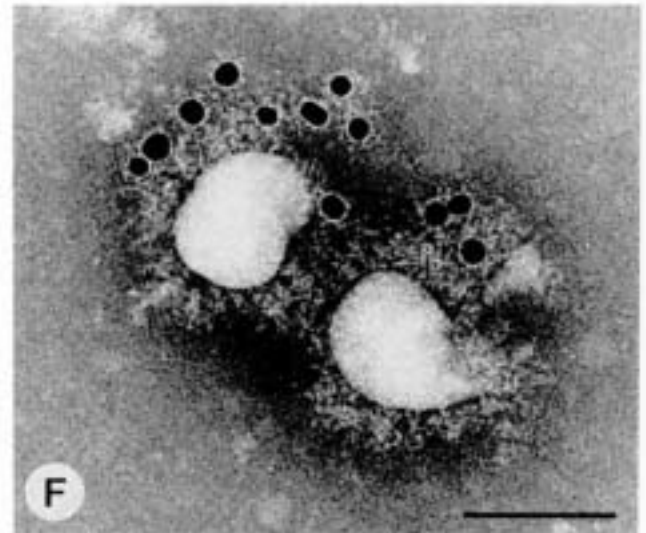
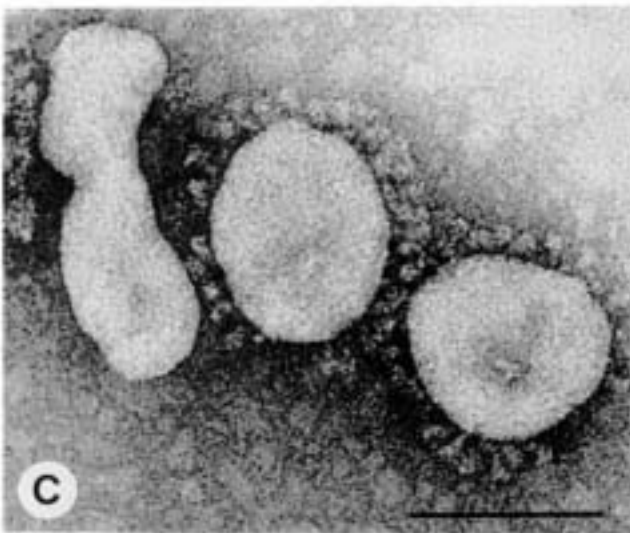
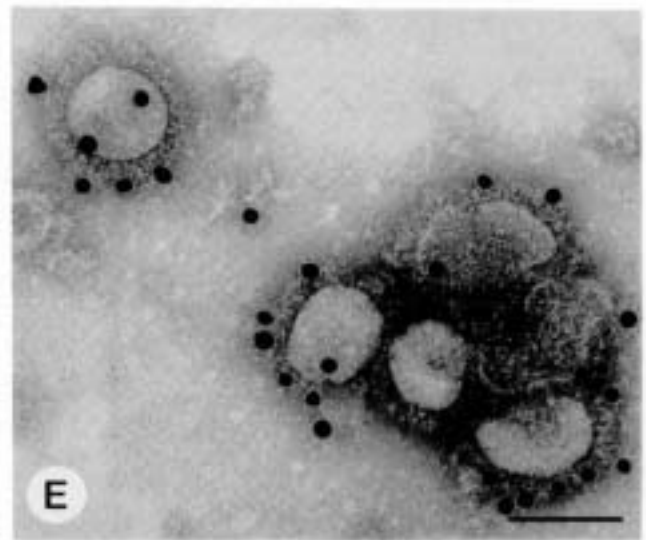
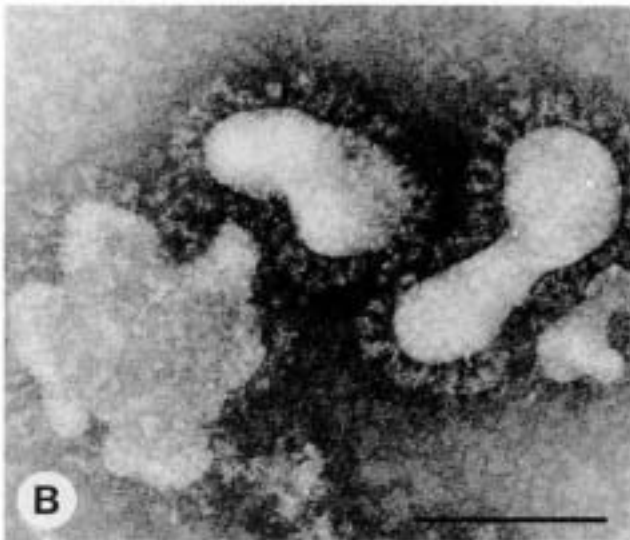
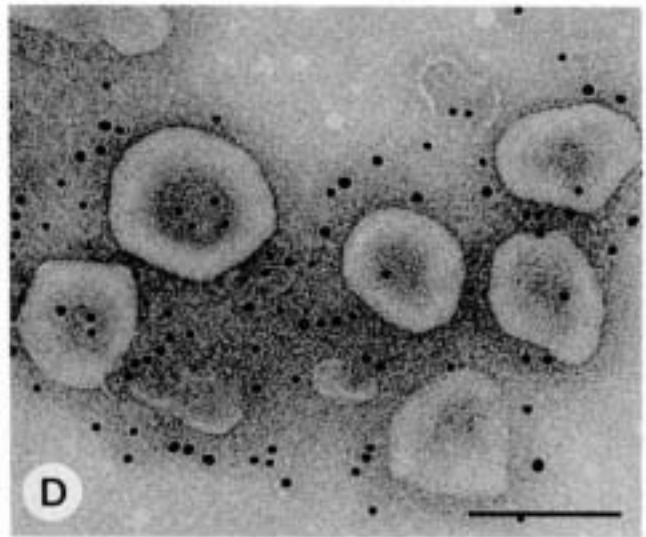
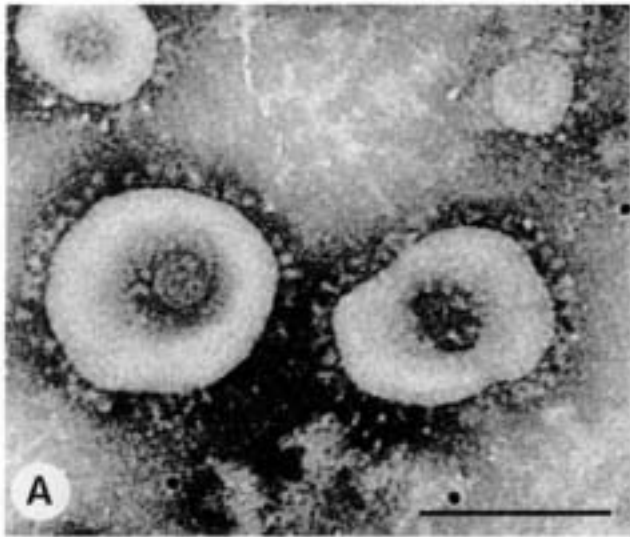
Mixing the various coronaviruses with their homologous antisera resulted in the appearance of virus-antibody aggregates containing up to 50 morphologically intact particles. Following incubation with the PAG complex, specific gold labeling was obtained (Figs. 1, 2). The gold granules were usually distributed around and between virus particles, near the tip of the surface projections, whereas the interior of the virions was not labeled. Only a few gold granules were observed around viral particles that had lost their surface peplomers. Occasionally, the surface projections appeared to be masked, probably by immunoglobulins (Figs. 1F, 2F). In the cases of hemagglutinating mammalian corona-

→

**Figure 1.** Avian and mammalian enteric coronaviruses. **A.** Negatively stained BCoV particles showing the double fringe of surface projections. The small granular projections were particularly well defined on the particles that lost their more typical coronaradiations. **B.** Negatively stained TCV particles, The TCV virions also possess 2 types of surface projections. Note the characteristic inner tongue-shaped structure of the coronaviruses. **C.** Negatively stained purified TGEV particles. The TGEV virions are very pleomorphic in size and shape and possess only 1 fringe of regularly spaced club-shaped projections. **D.** Protein A-immunogold labeling of purified BCoV particles after incubation with rabbit anti-BCoV hyperimmune serum. Most of the gold granules are closely associated with the viral particles, with minimal gold background staining. **E.** Protein A-immunogold labeling of the large peplomers of TCV virions after incubation with antiserum produced against the egg-adapted Minnesota strain of TCV. **F.** Specific immunogold labeling of a TGEV particle. The surface projections are masked by the presumably antigen-antibody fringe. Bars = 100 nm.







viruses and TCV, a double row of gold granules could be observed around the viral particles, probably corresponding to the 2 types of surface projections (Fig. 4A).

#### Sensitivity of DEM and PAG-IEM

To compare the sensitivity of both DEM and PAG-IEM methods, purified TCV and BCV preparations were first adjusted to approximately  $10^9$  viral particles per ml, as determined by DEM. calibration with latex spheres. At least 1-10 viral particles per grid square were still detectable in negative stained preparations at a 1:2,500-1:5,000 dilution of the initial viral suspensions. Using labeled virus particles as the end point, PAG-IEM was at least 10 times more sensitive than DEM. Using PAG-IEM, immunocomplexes (i.e., labeling of viral antigens of unrecognizable morphology or labeling of free peplomers) were still detectable at a  $10^{-5}$  dilution of the initial viral suspensions, and few if any aggregated coronavirions were detectable by DEM. below a virus concentration of  $10^6$  particles per ml.

#### Shared antigenic reactions among various coronaviruses as determined by PAG-IEM

In general, the anticoronavirus hyperimmune sera did not react by PAG-IEM with viruses belonging to the unrelated antigenic subgroups.<sup>16,20</sup> These antisera did not permit gold labeling of all viruses antigenically related to the parental virus. Two-way cross-antigenic relationships were demonstrated between BCV, HEV, and HCV-OC43, but heterologous antisera did not react against MHV-3 (Table 1). Similarly, antisera to IBV, MHV-3, and TGEV reacted only with their homologous virus, whereas anti-HCV-229E did not show any cross-reactivity with the other coronaviruses tested. The antiserum produced to the Beaudette strain of IBV reacted strongly with the 3 strains of IBV tested. Moreover, reciprocal antigenic relatedness was demonstrated between TCV, BCV, HCV-OC43, and HEV, but no reactivity was observed between TCV and the avian IBVs.

#### Detection of coronaviruses in clinical specimens from diarrheic calves and diarrheic turkey poult

By DEM, it was often difficult to visualize intact virions and differentiate these from other fringed bodies (Fig. 3A, 3B). These types of coronavirus-like par-

ticles were often observed, particularly in turkey fecal samples and allantoic fluids from embryonating hen eggs that were inoculated with tissue culture-adapted TCV isolates. The low numbers of virus particles and the presence of fecal debris compound these difficulties and made unequivocal diagnosis of the presence of coronaviruses difficult.

Virus particles were concentrated approximately 20-50 times by direct ultracentrifugation on the EM grids. The fecal background debris was markedly reduced but fringed bodies and virus-like particles also increased in number, making interpretation difficult. When PAG complexes were used as an electron-dense marker, gold particle background was twice as dense as that seen in partially purified virus stock, but specific labeling could readily be distinguished by comparison with controls where hyperimmune serum was omitted.

The use of the PAG complex permitted differentiation of damaged viral particles that otherwise might have been mistaken for membranous cellular materials (Fig. 4B). In many instances, only free peplomers or few peplomers still attached to the viral particles were labeled by the gold granules (Fig. 4C, 4D). Furthermore, because of their extreme electron density, the gold granules were readily observable at EM magnification as low as 10,000 x, allowing a large area of the grid to be scanned quickly. In the present study, 12 out of 20 and 20 out of 38 fecal samples from diarrheic calves and diarrheic turkey poult, respectively, were positive for coronavirus antigens by both PAG-IEM and indirect ELISA. The ELISA technique did not permit the identification of other positives among specimens tested from diarrheic poult, whereas two specimens (2/20) from diarrheic calves that were weakly positive by ELISA could not be confirmed by PAG-IEM.

### Discussion

In the last few years, several serologic methods, such as ELISA,<sup>2,5,22</sup> counterimmunoelectroosmophoresis,<sup>3</sup> and immunoelectron microscopy,<sup>18,24</sup> have been used for the detection of coronaviruses associated with neonatal gastroenteritis in farm animals. To be reliable and accurate, these tests require highly specific antisera or monoclonal antibodies.\* The presence of specific blocking antibodies in the intestinal secretions from coronavirus-infected animals may interfere with the

Figure 2. Avian and mammalian respiratory coronaviruses. A. Negatively stained purified IBV particles surrounded by a fringe of regularly spaced petal-shaped projections. B. Negatively stained purified HCV-OC43 particles. C. Negatively stained purified HEV particles. D. Protein A-immunogold labeling of purified IBV particles after incubation with anti-IBV rabbit hyperimmune serum. E. Protein A-immunogold labeling of purified HCV-OC43 virions after incubation with anti-HCV-OC43 hyperimmune serum. Two types of surface projections are seen on the damaged viral particles. F. Protein A-immunogold labeling of purified HEV virions after incubation with rabbit anti-HEV (strain 67N) serum. The surface projections are presumably masked by specific immunoglobulins. Bars = 100 nm.

Table 1. Cross-antigenic relationships between coronaviruses as determined by protein A-gold immunoelectron microscopy.

Antiserum	Viruses								
	BCV VR874	IBV Holland	IBV M41	IBV Mass.	TGE Purdue	MHV-3	TCV Minn.	HEV 67N	HCV-OC43
BCV VR874	+++*	-	-	-	-	-	+++	++	++
IBV Beau.	-	+++	+++	+++	-	-	-	-	-
TGE Purdue	-	-	-	-	++	-	-	-	-
MHV-3	-	-	-	-	-	+++	+	ND	ND
TCV Minn.	+++	-	-	-	-	-	+++	++	++
HEV 67N	+++	-	-	-	-	ND	+++	+++	+
HCV-OC43	++	ND	ND	-	-	ND	+	+	+++
HCV-229E	-	-	-	-	-	-	-	ND	ND

+, ++, +++ indicate relative intensity of gold labeling; - = negative; ND = not done.

reaction, giving rise to false-negative results. Furthermore, proteases in clinical specimens can dissociate the immunoreactants from solid-phase surfaces, therefore decreasing the sensitivity of the ELISA.<sup>27</sup>

Detection of the pleomorphic coronavirus particles in clinical specimens, such as respiratory secretions and stools, was initially done by DEM, although failure to preserve surface projections and the presence of particles that morphologically resemble coronaviruses make DEM less suitable for precise identification of coronavirus-positive or -negative specimens.<sup>10,11</sup> Prior investigations confirmed that when fecal samples containing BCV or TCV were examined by DEM coronavirus particles were usually widely spaced and the background heavily contaminated with debris.<sup>3,5</sup> Fringed particles that could be mistaken for coronaviruses were frequently observed, particularly in cases of specimens obtained from diarrheic turkey poults.<sup>5,23</sup>

In the present study, PAG-IEM coupled to direct

airfuge ultracentrifugation of samples on EM grids proved to be a rapid, simple, and sensitive test for detection, identification, and ultrastructural studies of coronavirus particles or their subunits. As previously reported,<sup>1,15</sup> direct ultracentrifugation of samples on an EM specimen grid increased the sensitivity and quality of preparations. Both density gradient fractions and clarified clinical samples could be easily washed, leaving a much cleaner background. The inclusion of the specimen grid directly in the tube ensures that all viral particles and subunits are deposited on the grid, thus increasing the sensitivity. This approach proved satisfactory with minimal distortion of the specimen during centrifugation. Distribution of samples was also relatively even on the grid.

Immunogold labeling improved the detection of coronaviruses in clinical specimens by increasing specificity and sensitivity. The PAG-IEM method was applicable to detection of coronavirus particles or antigens

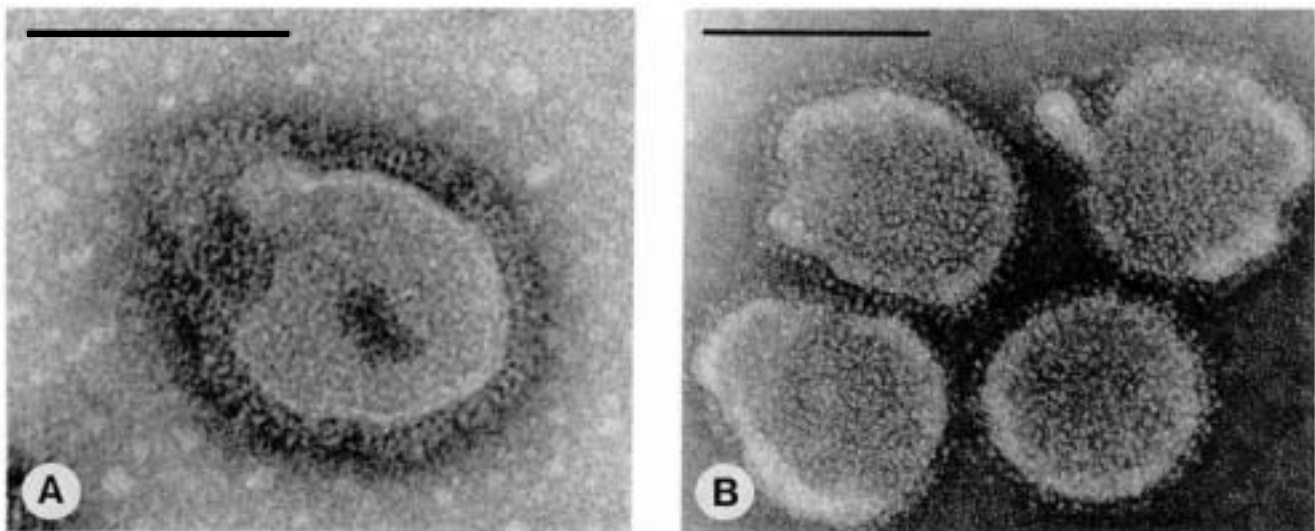


Figure 3. Coronavirus-like particles in the feces of diarrheic turkey poults. A, B. Fringed bodies were frequently visualized by DEM of avian fecal samples. These particles, which may have been mistaken for coronaviruses, were not gold labeled following incubation with anti-TCV and anti-IBV hyperimmune sera. Bars = 100 nm.



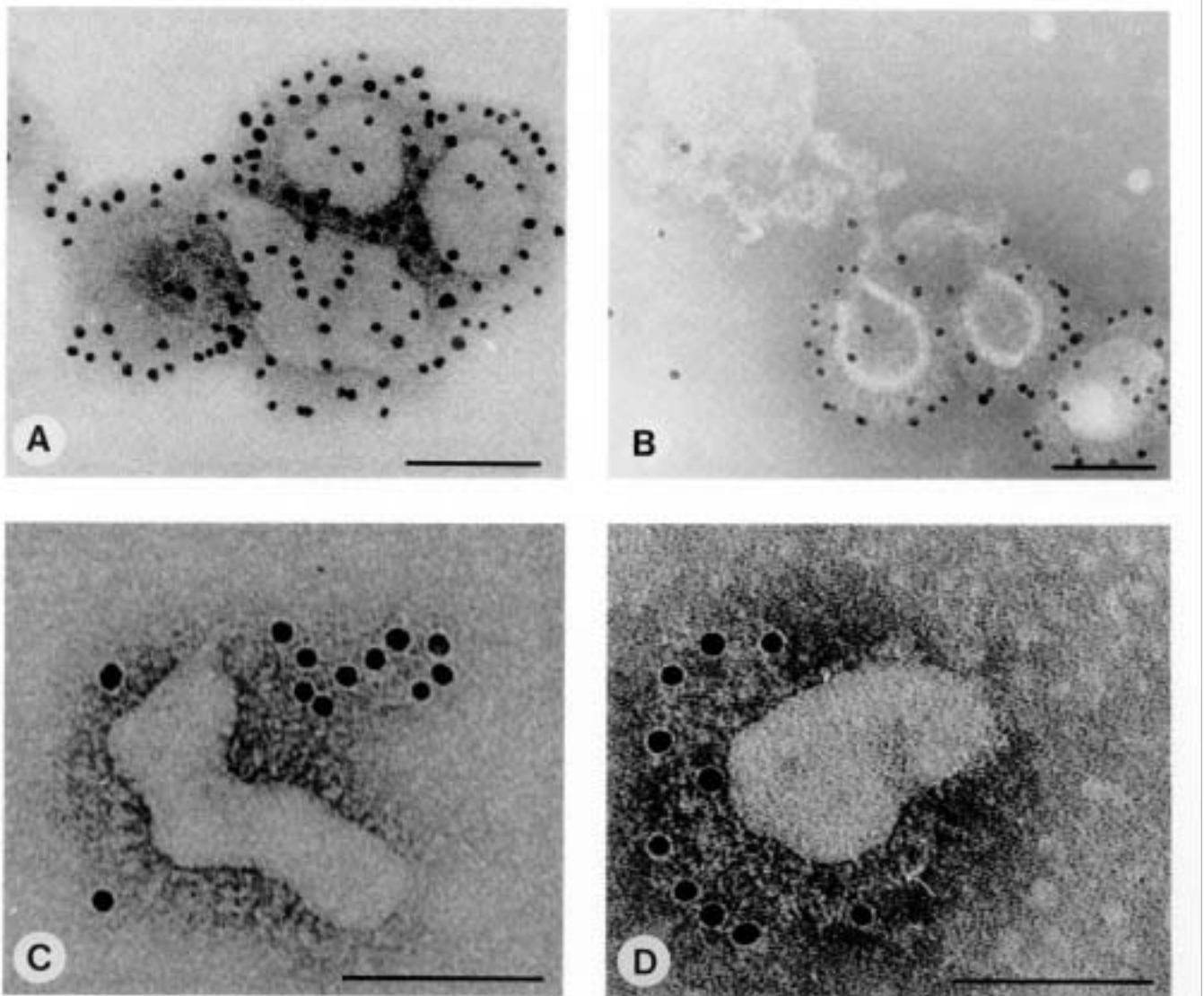


Figure 4. PAG-IEM of intact and damaged TCV particles in the feces of diarrheic turkey poult. **A.** Two rows of gold granules, corresponding to the 2 types of surface projections, were occasionally observed around TCV particles. **B.** Without gold labeling, these TCV particles would have been mistaken for cell artifacts. **C, D.** Specific gold labeling of soluble (free peplomers) as well as particle-associated antigen after incubation with anti-TCV hyperimmune serum. Note the absence of gold background staining. Bars = 100 nm.

in both purified preparations and stool suspensions. Sensitivity for coronavirus detection in stools of PAG-IEM was 10-50 times higher than that of DEM. The sensitivity was increased in 2 ways. First, incubation of clinical samples with hyperimmune serum often led to a specific aggregation of the coronaviral particles. Second, The PAG-IEM method permitted detection of soluble and particle-associated antigens. Many particles that were interpreted initially as membranous material or fringed cellular debris by DEM were identified as damaged coronavirus particles because of the specific labeling by the PAG complex of surface projections still attached on these membranes or free in the supernatant fluid. Numerous fringed particles that

were mistaken for coronavirus particles could also be discriminated by PAG-IEM. In preliminary experiments with purified viral preparations, PAG-IEM detecting label alone (i.e., labeling of viral antigens of unrecognizable morphology or labeling of free peplomers) was as sensitive as indirect ELISA (data not shown).

Careful attention to the concentration of both antiserum and PAG was important in maintaining a high degree of specific labeling. Excess antibody resulted in excessive labeling; the optimum dilution of each reference antiserum used varied from 1:250 to 1:1,000 (original ELISA titer ranged from 1:12,800 to 1:102,400).

Investigations of the cross-antigenic relationships between various coronaviruses by PAG-IEM revealed the close antigenic relationship between bovine and turkey enteropathogenic coronaviruses, in agreement with previous findings by ELISA and Western immunoblotting with tissue culture-adapted and egg-adapted TCV isolates.<sup>5,7</sup> Both viruses possess an hemagglutinating activity that has been associated to a 140-kD envelope glycoprotein (a disulfide-linked dimer) and additional small granular surface projections located near the base of the typical large bulbous peplomers of the coronavirions.<sup>4,6</sup> Both viruses are also antigenically related to the porcine HEV and human HCV-OC43 coronaviruses, 2 other viruses that belong to the subgroup of mammalian hemagglutinating coronaviruses. Previous studies have demonstrated that these viruses all share antigenic determinants located on their homologous structural proteins.<sup>7,16</sup> The morphologic and serologic homologies among the viruses belonging to this subgroup of coronaviruses, except for MHV-3, was well demonstrated using the PAG-IEM method. No cross-reactivity was demonstrated between the hemagglutinating coronaviruses and TGEV, HCV-229E, and IBV, belonging to 2 other serologic subgroups of coronaviruses. Data obtained by PAG-IEM thus helps confirm the serologic classification of coronaviruses that was originally established on the basis of results obtained by indirect immunofluorescence and ELISA.<sup>5,13,20,26</sup>

Recently, molecular hybridization studies with cDNA probes holding sequences from the N and M genes of TGEV and BCV also permitted identification of coronaviruses that were antigenically closely related to the parental virus but not of the coronaviruses belonging to an antigenically unrelated subgroup.<sup>25</sup> Only a weak hybridization signal was obtained using BCV cDNA probes against MHV-3. Genomic relatedness between BCV and TCV has also been demonstrated by this molecular hybridization, and reclassification of TCV in the subgroup of mammalian hemagglutinating coronaviruses has been proposed.<sup>7</sup>

In conclusion, the combined use of direct ultracentrifugation of samples on EM grids and PAG-IEM techniques for the routine examination of clinical samples from diarrheic animals is recommended. This approach is technically rapid, simple, and highly reproducible and provides increased sensitivity and better contrast.

### Acknowledgements

We greatly appreciate the technical assistance of J. Beaubien and H. Strykowski. This study was partly supported by grants from the National Research Council of Canada (NSERC) and the FCAR Quebec.

### Sources and manufacturers

- a. Dr. B. S. Pomeroy, College of Veterinary Medicine, St. Paul, MN.
- b. Bovine crystallized trypsin, grade XIII, Sigma Chemical Co., St. Louis, MO.
- c. American Type Culture Collection, Rockville, MD.
- d. Philips EM 300, Eindhoven, The Netherlands.
- e. Airfuge, rotor model A-100, Beckmann Instruments, Palo Alto, CA.
- f. Centrifuge model RC-2B, rotor model SS34, Ivan Sorval, Newton, CT.

### References

1. Alain R, Nadon F, Seguin C, et al.: 1987, Rapid virus subunit visualization by direct sedimentation of samples on electron microscopic grids. *J Virol Methods* 16:209-216.
2. Crouch CF, Raybould TJG, Acres SD: 1984, Monoclonal antibody capture enzyme-linked immunosorbent assay for detection of bovine enteric coronavirus. *J Clin Microbiol* 19:388-393.
3. Dea S, Roy RS, Begin ME: 1979, Counterimmunoelectrophoresis for detection of neonatal calf diarrhea coronavirus: methodology and comparison with electron microscopy. *J Clin Microbiol* 10:240-244.
4. Dea S, Tijssen P: 1989, Antigenic and polypeptide structure of turkey enteric coronaviruses as defined by monoclonal antibodies. *J Gen Virol* 70: 1725-1741.
5. Dea S, Tijssen P: 1989, Detection of turkey enteric by enzyme-linked immunosorbent assay and differentiation from other coronaviruses. *Am J Vet Res* 50:226-231.
6. Dea S, Tijssen P: 1989, Isolation and trypsin-enhanced propagation of turkey enteric (bluecomb) coronaviruses in a continuous human rectal tumor (HRT-18) cell line. *Am J Vet Res* 50: 1310-1318.
7. Dea S, Verbeek AJ, Tijssen P: 1990, Antigenic and genomic relationships among turkey and bovine enteric coronaviruses. *J Virol* 64:3112-3118.
8. De Mey J: 1983, Colloidal gold probes in immunocytochemistry. *In: Immunocytochemistry: applications in pathology and biology*, ed. Polak J, Van Noordens S, pp. 82-113. J. Wright and Sons, London, England.
9. El-Ghorr AA, Snodgrass DR, Scott FMM: 1988, Evaluation of an immunogold electron microscopy technique for detecting bovine coronavirus. *J Virol Methods* 19:215-224.
10. Eugster AK, Sneed L: 1980, Viral intestinal infections of animals and man. *Comp Immun Microbiol Infect Dis* 2:417-435.
11. Flewett TH: 1978, Electron microscopy in the diagnosis of infectious diarrhea. *J Am Vet Med Assoc* 173:538-543.
12. Frens G: 1973, Controlled nucleation for the regulation of the particle size in monodisperse gold suspension. *Nature (Phys. Sci.)* 241:20-22.
13. Gerna G, Cereda PM, Grazia-Revello M, et al.: 1981, Antigenic and biological relationships between human coronavirus OC43 and neonatal calf diarrhoea coronavirus. *J Gen Virol* 54:91-102.
14. Gibbs EPJ, Smale CJ, Voyle CA: 1980, Electron microscopy as an aid to the rapid diagnosis of virus diseases of veterinary importance. *Vet Rec* 106:451-458.
15. Hammond GW, Hazelton PR, Chuang I, et al.: 1981, Improved detection of viruses by electron microscopy after direct ultracentrifuge preparation of specimen. *J Clin Microbiol* 14:210-221.
16. Hogue BG, King B, Brian DA: 1984, Antigenic relationships among proteins of bovine coronavirus, human respiratory co-



- ronavirus OC 43, and mouse hepatitis coronavirus A59. *J Virol* 51:384-388.
17. Hopley JFA, Doane FW: 1985, Development of a sensitive protein A-gold immunoelectron microscopy method for detecting viral antigens in fluid specimens. *J Virol Methods* 12: 135-147.
  18. Jensen MT, Kemeny LJ, Stone SS, et al.: 1980, Direct immunoelectron microscopy of transmissible gastroenteritis virus with immunoglobulins G and A and guinea pig complement. *Am J Vet Res* 41:136-139.
  19. Mebus CA, Newman LE, Stair EL: 1975, Scanning electron, light, and immunofluorescent microscopy of intestine of gnotobiotic calf infected with calf diarrheal coronavirus. *Am J Vet Res* 36:1719-1725.
  20. Pedersen NC, Ward I, Mengeling WL: 1978, Antigenic relationships of the feline infectious peritonitis virus to coronaviruses of other species. *Arch Virol* 58:45-53.
  21. Pomeroy KA, Patel BL, Larsen CT, et al.: 1978, Combined immunofluorescence and transmission electron microscopic studies of sequential intestinal samples from turkey embryos and poultz infected with turkey enteritis coronavirus. *Am J Vet Res* 39: 1348-1354.
  22. Reynolds DJ, Chasey D, Scott AC, et al.: 1984, Evaluation of ELISA and electron microscopy for the detection of coronavirus and rotavirus in bovine faeces. *Vet Rec* 114:397-401.
  23. Ritchie AE, Deshmukh DR, Larsen CT, et al.: 1973, Electron microscopy of coronavirus-like particles characteristic of turkey bluecomb disease. *Avian Dis* 17: 546-558.
  24. Saif LJ, Bohl EH, Kohler EM, et al.: 1977, Immune electron microscopy of transmissible gastroenteritis virus and rotavirus (reovirus-like agent) of swine. *Am J Vet Res* 38: 13-20.
  25. Shockley LJ, Kapke PA, Lapps W, et al.: 1987, Diagnosis of porcine and bovine enteric coronavirus infections using cloned cDNA probes. *J Clin Microbiol* 25: 1591-1596.
  26. Siddell S, Wege H, der Meulen V: 1983, The biology of coronaviruses. *J Gen Virol* 64:761-776.
  27. Viscidi R, Laughon BE, Hanvanich M, et al.: 1984, Improved enzyme immunoassays for the detection of antigens in fecal specimens: investigation and correction of interfacing factors. *J Immunol Methods* 67: 129-143.